Optical polarization properties of *M*-plane GaN films investigated by transmittance anisotropy spectroscopy

Jayeeta Bhattacharyya, Sandip Ghosh,[a] and B. M. Arora
Department of Condensed Matter Physics and Material Science, Tata Institute of Fundamental Research, Homi Bhabha Road, Mumbai 400005, India

O. Brandt and H. T. Grahn
Paul-Drude-Institut für Festkörperelektronik, Hausvogteiplatz 5-7, 10117 Berlin, Germany

(Received 29 August 2007; accepted 24 November 2007; published online 20 December 2007)

The authors investigate the in-plane optical polarization properties of $[1\bar{1}00]$-oriented (*M*-plane) GaN films on γ-$LiAlO_2$(100) substrates by transmittance anisotropy spectroscopy (TAS). This technique is sensitive to the difference in the transmittance between light polarized parallel and perpendicular to the *c* axis of GaN, which for *M*-plane GaN lies in the film plane. The TAS spectrum exhibits a clear resonance in the vicinity of the fundamental bandgap. Simulations demonstrate that this resonance directly reflects the polarization-dependent shift of the bandgap. The zero crossings of the differential TAS spectrum are shown to be a measure for the polarization-dependent transition energies. © *2007 American Institute of Physics*. [DOI: 10.1063/1.2824841]

Group-III nitride semiconductor films of nonpolar orientations, such as *M*-plane $(1\bar{1}00)$ and *A*-plane $(11\bar{2}0)$ films, as indicated in the inset of Fig. 1(a), are promising candidates for optoelectronic device applications. The absence of large piezo- and pyroelectric fields in group-III nitride quantum wells grown with such orientation[1] has opened up the possibility of producing highly efficient[2–5] and polarized[6] light emitters, including lasers.[7–9] *M*-plane films have also been used for realizing novel devices such as polarization-sensitive photodetectors,[10] very narrow-band photodetection configurations,[11] and Bragg-reflector-based polarization switches.[12] *M*- and *A*-plane films, typically grown on $LiAlO_2$, sapphire, and SiC, experience strain values of different magnitudes along directions parallel (‖) and perpendicular (⊥) to the *c* axis of GaN, which for *M*- and *A*-plane GaN lies in the film plane. This anisotropic strain can drastically modify the polarization selection rules for interband transitions, resulting in large polarization-dependent shifts of the corresponding bandgaps. Therefore, the characterization of these interband transitions in terms of their energies and polarization selection rules is vitally important for the development of polarization-sensitive devices.

For this type of characterization, polarized transmittance,[13] reflectance,[14] and photoreflectance[15] spectroscopy have been utilized, each requiring two measurements with the electric field $\boldsymbol{E}\perp\boldsymbol{c}$ and $\boldsymbol{E}\parallel\boldsymbol{c}$. Reflectance anisotropy spectroscopy (RAS) is an example of a modulation technique that gives information on the in-plane polarization anisotropy and involves only a single measurement. In fact, RAS has been extensively used to study the in-plane polarization properties of III-V semiconductors.[16] However, the RAS line shapes measured on thin films are strongly influenced by optical interference effects. Therefore, RAS can only be used at energies much larger than the bandgap, where strong absorption ensures the absence of thin-film interference fringes. We propose instead the application of transmittance anisotropy spectroscopy (TAS) to study the optical polarization properties in thin *M*-plane GaN films in the vicinity of the fundamental bandgap. We compare the measured TAS spectral line shapes with results of polarized absorption measurements and simulations. An empirical method to extract the excitonic transition energies is presented.

The *M*-plane GaN films were grown by rf plasma-assisted molecular beam epitaxy on γ-$LiAlO_2$(100) substrates.[17] We focus on the results obtained on a 0.45 μm thick sample. High-resolution x-ray diffractometry demon-

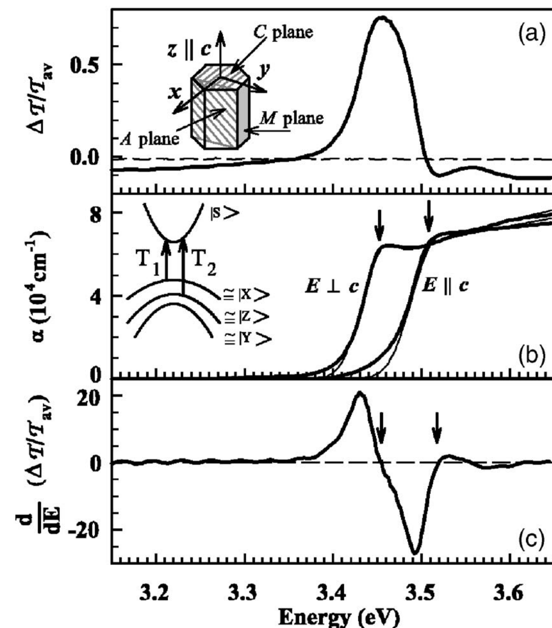

FIG. 1. (a) TAS spectrum of the 0.45 μm thick *M*-plane GaN film (solid line) and the $LiAlO_2$ substrate (dashed line) at 297 K. The inset shows the unit cell of wurtzite GaN. (b) Measured (thick lines) and simulated (thin lines) absorption spectra for $\boldsymbol{E}\perp\boldsymbol{c}$ and $\boldsymbol{E}\parallel\boldsymbol{c}$. The inset shows schematically the band structure of GaN under overall compressive anisotropic strain in the *M*-plane. The arrows mark the transition energies E_{T_1} and E_{T_2}. (c) First derivative of the TAS spectrum in (a). The dashed line marks zero magnitude, the arrows the zero crossings.

a)Electronic mail: sangho10@tifr.res.in.

 © 2007 American Institute of Physics
Author complimentary copy. Redistribution subject to AIP license or copyright, see http://apl.aip.org/apl/copyright.jsp

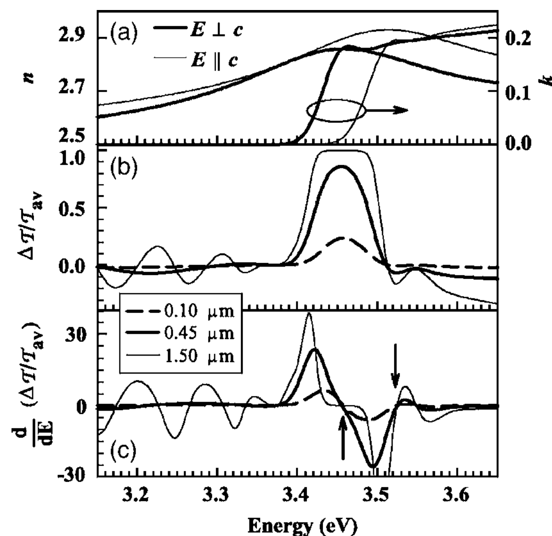

FIG. 2. (a) Real (n) and imaginary (k) part of the refractive index of GaN for $\boldsymbol{E} \perp \boldsymbol{c}$ and $\boldsymbol{E} \parallel \boldsymbol{c}$ as used in the simulation of the 297 K spectra. (b) Simulated TAS spectra of M-plane GaN films for three different thicknesses. (c) First derivative of the three TAS spectra in (b). The arrows indicate the zero crossings.

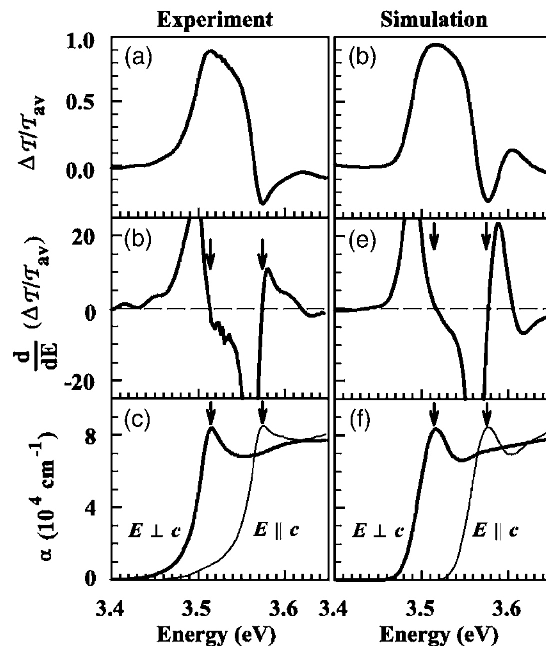

FIG. 3. (a) Measured and (d) simulated TAS spectrum of the 0.45 μm thick M-plane GaN film at 8 K. First derivative of the (b) measured and (e) simulated TAS spectrum in (a) and (d), respectively. The dashed lines mark zero magnitude, the arrows the zero crossings. (c) Measured and (f) simulated absorption spectra at 8 K for $\boldsymbol{E} \parallel \boldsymbol{c}$ and $\boldsymbol{E} \perp \boldsymbol{c}$. The arrows mark the transition energies E_{T_1} and E_{T_2}.

strates that the film is under in-plane biaxial compressive strain with an out-of-plane dilation of $\epsilon_{yy}=0.39\%$. The transmittance ($\mathcal{T}$) measurements were performed using a Xe lamp and a grating monochromator (MC). To ensure unpolarized light, the output of the MC was sent through a quartz-wedge depolarizer. The probe beam was obtained by passing this unpolarized light through a Glan-Taylor polarizer, which was continuously rotated with a frequency $f_p=7.5$ Hz. Phase sensitive detection was performed using an UV-enhanced Si photodiode and a lock-in amplifier (LIA) locked to $2f_p$. To properly set the initial phase ϕ_{LIA}, the sample is replaced by a second polarizer with its polarization axis parallel to the MC slits, and ϕ_{LIA} is adjusted to obtain a maximum in-phase output signal. If the sample is now placed with the c axis parallel to the MC slits, the ac signal amplitude is proportional to the TAS signal $\Delta\mathcal{T}=[\mathcal{T}_{\boldsymbol{E}\parallel\boldsymbol{c}}-\mathcal{T}_{\boldsymbol{E}\perp\boldsymbol{c}}]/2$. The separately measured dc signal from the photodiode is proportional to the average transmittance $\mathcal{T}_{\mathrm{av}}=[\mathcal{T}_{\boldsymbol{E}\parallel\boldsymbol{c}}+\mathcal{T}_{\boldsymbol{E}\perp\boldsymbol{c}}]/2$ and used to normalize the TAS signal. The polarized absorption spectra were obtained from transmission measurements with the polarizer oriented either parallel or perpendicular to the c axis.

Figure 1(a) shows the room-temperature TAS spectrum of the M-plane GaN film (solid line), which exhibits a resonance around 3.45 eV. The TAS spectrum of the bare substrate, indicated by the dashed line in Fig. 1(a), is featureless and sets the baseline. In order to understand the origin of the TAS spectrum of the M-plane GaN film, we separately determined the absorption spectrum α for $\boldsymbol{E} \perp \boldsymbol{c}$ and $\boldsymbol{E} \parallel \boldsymbol{c}$ marked by the thick lines in Fig. 1(b). For $\boldsymbol{E} \parallel \boldsymbol{c}$, the absorption edge clearly shifts to higher energies. Therefore, the predominantly positively peaked TAS resonance arises from this polarization-dependent bandgap shift, which results in a large relative change of the transmittance in the energy range where the absorption is high for $\boldsymbol{E} \perp \boldsymbol{c}$ and low for $\boldsymbol{E} \parallel \boldsymbol{c}$. These two bandgaps originate from transitions between the two uppermost valence bands (VBs) and the conduction band as indicated by T_1 and T_2 in the inset of Fig. 1(b). For a sufficiently large anisotropic strain in M-plane GaN films, the symmetry of the two uppermost VBs becomes predominantly $|X\rangle$- and $|Z\rangle$-like. Therefore, the T_1 and the T_2 transitions are mainly x and z polarized, respectively. The two excitonic transition energies $E_{T_1}=3.45$ eV and $E_{T_2}=3.507$ eV for $\boldsymbol{E} \perp \boldsymbol{c}$ and $\boldsymbol{E} \parallel \boldsymbol{c}$, respectively, are obtained from fitting the experimental spectra to simulated absorption spectra indicated by the thin lines in Fig. 1(b). The simulations included the Sommerfield enhancement factor and a Gaussian-broadened excitonic resonance with full width at half maximum (FWHM) of 53 meV. Figure 1(c) shows the first derivative of the TAS spectrum, where the zero crossings at 3.455 and 3.518 eV of the dominant negative lobe are located slightly above (within 11 meV) of the energies E_{T_1} and E_{T_2}.

In order to quantitatively analyze the line shape of the TAS spectrum, we have performed simulations using the transfer matrix approach. Figure 2(a) shows the real (n) and imaginary (k) part of the refractive index of the GaN film for $\boldsymbol{E} \parallel \boldsymbol{c}$ and $\boldsymbol{E} \perp \boldsymbol{c}$, which are used for the simulations of the room temperature spectra. k was derived from the measured absorption spectra, while n was obtained using the data in Ref. 18. The Kramers-Kronig compatibility of these two data sets was checked. For $LiAlO_2$, which is transparent in this energy range, n was taken to be 1.601 and 1.620 for $\boldsymbol{E} \perp \boldsymbol{c}$ and $\boldsymbol{E} \parallel \boldsymbol{c}$, respectively (note that $\boldsymbol{c}_{\mathrm{LiAlO_2}} \perp \boldsymbol{c}_{\mathrm{GaN}}$). Figure 2(b) shows the simulated TAS spectra for three different GaN film thicknesses. The simulation for the 0.45 μm thick film matches the measured spectrum in Fig. 1(a) quite well. Figure 2(c) displays the first derivative of the simulated TAS spectra. Note that the zero crossings of the dominant negative lobe at 3.455 and 3.520 eV are independent of the film thickness. By measuring a second sample with a thickness of 1.2 μm, we have verified the close correlation between the zero crossings and the actual transition energies E_{T_1} and E_{T_2}. Figure 3(a) shows the TAS spectrum of the 0.45 μm thick

Author complimentary copy. Redistribution subject to AIP license or copyright, see http://apl.aip.org/apl/copyright.jsp

film recorded at 8 K. The zero crossings of the dominant negative lobe of the first derivative of the TAS spectrum shown in Fig. 3(b) are at 3.512 and 3.572 eV, which are identical within experimental accuracy to the transition energies E_{T_1} and E_{T_2} obtained from the absorption spectra in Fig. 3(c). Note that the exciton resonance is considerably sharper (FWHM=38 meV) than at room temperature. Thus, for sufficiently narrow resonances, the zero crossings can be used as an accurate measure of the transition energies. The simulated line shapes in Figs. 3(d)–3(f) also agree very well with the measured spectra. We have used the Bir-Pikus Hamiltonian[15] to calculate the effect of anisotropic strain on the transition energies using the parameters listed in Refs. 19 and 20. The measured transition energies at low temperatures correspond to strain values of $\epsilon_{xx} \simeq -1.1\%$ and $\epsilon_{zz} \simeq -0.4\%$.

In conclusion, we have shown how transmission anisotropy spectroscopy can be used to obtain important information on the transition energies and polarization properties of *M*-plane GaN films. A single TAS measurement can be used for a rapid, postgrowth, room-temperature characterization of group-III nitride films of nonpolar orientations. From the device point of view, E_{T_1} gives the emission energy for a polarized light source based on an *M*-plane GaN film. A positive (negative) sign of the main TAS resonance indicates that the emission polarization direction would be $\boldsymbol{E} \perp \boldsymbol{c}$ ($\boldsymbol{E} \parallel \boldsymbol{c}$). By comparison with fabricated devices, we find that the working range for polarization-sensitive photodetectors and narrow-band photodetection configurations can be directly obtained from the width of the dominant TAS resonance with the peak response being centered close to E_{T_1}.

The authors would like to thank R. Averbeck and H. Riechert for their support in growing one of the films. One of the authors (S.G.) acknowledges useful discussions with G. Adhikary and A. Bhattacharya.

[1] P. Waltereit, O. Brandt, A. Trampert, H. T. Grahn, J. Menniger, M. Ramsteiner, M. Reiche, and K. H. Ploog, Nature (London) **406**, 865 (2000).
[2] M. D. Craven, P. Waltereit, J. S. Speck, and S. P. DenBaars, Appl. Phys. Lett. **84**, 496 (2004).
[3] T. Koida, S. F. Chichibu, T. Sota, M. D. Craven, B. A. Haskell, J. S. Speck, S. P. DenBaars, and S. Nakamura, Appl. Phys. Lett. **84**, 3768 (2004).
[4] A. Chakraborty, B. A. Haskell, H. Masui, S. Keller, J. S. Speck, S. P. DenBaars, S. Nakamura, and U. K. Mishra, Jpn. J. Appl. Phys., Part 1 **45**, 739 (2006).
[5] K.-C. Kim, M. C. Schmidt, H. Sato, F. Wu, N. Fellows, M. Saito, K. Fujito, J. S. Speck, S. Nakamura, and S. P. DenBaars, Phys. Status Solidi (RRL) **1**, 125 (2007).
[6] N. F. Gardner, J. C. Kim, J. J. Wierer, Y. C. Shen, and M. R. Krames, Appl. Phys. Lett. **86**, 111101 (2005).
[7] H. Teisseyre, C. Skierbiszewski, A. Khachapuridze, A. Feduniewicz-Źmuda, M. Siekacz, B. Łucznik, G. Kamler, M. Kryśko, T. Suski, P. Perlin, I. Grzegory, and S. Porowski, Appl. Phys. Lett. **90**, 081104 (2007).
[8] K. Okamoto, H. Ohta, S. Chichibu, J. Ichihara, and H. Takasu, Jpn. J. Appl. Phys., Part 2 **46**, L187 (2007).
[9] M. C. Schmidt, K. C. Kim, R. M. Farrell, D. F. Feezell, D. A. Cohen, M. Saito, K. Fujitoi, J. S. Speck, S. P. Denbaars, and S. Nakamura, Jpn. J. Appl. Phys., Part 2 **46**, L190 (2007).
[10] C. Rivera, J. L. Pau, E. Muñoz, P. Misra, O. Brandt, H. T. Grahn, and K. H. Ploog, Appl. Phys. Lett. **88**, 213507 (2006).
[11] S. Ghosh, C. Rivera, J. L. Pau, E. Muñoz, O. Brandt, and H. T. Grahn, Appl. Phys. Lett. **90**, 091110 (2007).
[12] D. M. Schaadt, O. Brandt, S. Ghosh, T. Flissikowski, U. Jahn, and H. T. Grahn, Appl. Phys. Lett. **90**, 231117 (2007).
[13] S. Ghosh, P. Waltereit, O. Brandt, H. T. Grahn, and K. H. Ploog, Appl. Phys. Lett. **80**, 413 (2002).
[14] A. Alemu, B. Gil, M. Julier, and S. Nakamura, Phys. Rev. B **57**, 3761 (1998).
[15] S. Ghosh, P. Waltereit, O. Brandt, H. T. Grahn, and K. H. Ploog, Phys. Rev. B **65**, 075202 (2002).
[16] P. Weightman, D. S. Martin, R. J. Cole, and T. Farrell, Rep. Prog. Phys. **68**, 1251 (2005).
[17] P. Waltereit, O. Brandt, M. Ramsteiner, R. Uecker, P. Reiche, and K. H. Ploog, J. Cryst. Growth **218**, 143 (2000).
[18] T. Kawashima, H. Yoshikawa, S. Adachi, S. Fuke, and K. Ohtsuka, J. Appl. Phys. **82**, 3528 (1997).
[19] P. Misra, U. Behn, O. Brandt, H. T. Grahn, B. Imer, S. Nakamura, S. P. DenBaars, and J. S. Speck, Appl. Phys. Lett. **88**, 161920 (2006).
[20] The deformation potentials are $\alpha_{CB}=-44.5$ eV, $D_1=-41.4$ eV, $D_2=-33.3$ eV, and $D_5=-3.6$ eV. The crystal-field and spin-orbit splitting energies are $\Delta_{cr}=\Delta_1=9.2$ meV and $\Delta_{so}=3\Delta_2=18.9$ meV. The other parameters are obtained under the quasicubic approximation. The exciton binding energies are taken to be 26 meV. The energy of the unstrained *A*-exciton transition is taken to be 3.479 eV at 8 K. The elastic constants are $C_{11}=390$ GPa, $C_{12}=145$ GPa, $C_{13}=106$ GPa, and $C_{33}=398$ GPa.

Author complimentary copy. Redistribution subject to AIP license or copyright, see http://apl.aip.org/apl/copyright.jsp